Mechanism of ribosome translocation along messenger RNA

Yunxin Zhang*

Laboratory of Mathematics for Nonlinear Science,

Shanghai Key Laboratory for Contemporary Applied Mathematics, Centre for Computational Systems Biology,

School of Mathematical Sciences, Fudan University, Shanghai 200433, China.

(Dated: June 4, 2019)

In cells, helicase translocation along nucleic acid is essential for many biological processes. However, so far, the mechanism of this translocation is not fully understood. Recent studies show that helicase might translocate through two processes, active process and passive process, with different translocation rate. In this study, a mechanochemical model including such two processes is presented for ribosome translocation along messenger RNA during translation. In which, each of the two processes consists of two sub-processes, *translocation factor binding* sub-process and the following *mechanochemical* sub-process in which ribosome makes a forward translocation step. Ribosome switches stochastically between these two processes with external force dependent rates. By this model, we found that, with the increase of external force, the mean translocation rate of ribosome increases from one lower limit to another upper limit, and both of these two limits increase with concentrations of the translocation factors. Under high external force, ribosome translocates mainly through active process. At saturating concentration of translocation factors, the translocation is limited by *mechanochemical* sub-processes.

arXiv:1205.5026v1 [q-bio.BM] 23 May 2012

I. INTRODUCTION

In many biological events, such as replication, recombination and repair, double-stranded nucleic acid, i.e. DNA or RNA, should be firstly unwound to provide single-stranded template [1–6]. In this process, using the energy released from ATP hydrolysis helicase translocates along one strand of the double helix to unwind the nucleic acid [6–12]. Single molecule experiments found that the translocation rate of helicase along nucleic acid depends on the stability of base pairs (GC or AU base pair), the external force (which can be applied by optical tweezers assay or flow stretching assay), and the concentrations of translocation factors, such as EF-G, EF-Tu and ATP [13–21]. The translocation of helicase along nucleic acid might be active (in which the helicase acts as a strong molecular motor which converts chemical energy from ATP hydrolysis to unzip a duplexed template with high efficiency) or passive (in which helicase only can translate to the next base after the thermal fluctuation induced opening of the adjacent base pair) [5, 6, 11, 20, 22, 23]. So far, many models have been established to describe this unwinding process [11, 22, 24–34].

In this study, similar as in the description of dynamics of microtubules [35, 36], a two-process model will be presented for ribosome translocation along messenger RNA (mRNA) during translation. In which, ribosome translocates along

*Email: xyz@fudan.edu.cn

mRNA by either active process or passive process. During translocation, ribosome switches stochastically between these two processes, and the switch rate from passive process to active process depends on external force. Each process consists of two sub-processes: the *translocation factors* (EF-G•GTP and EF-Tu•GTP•aa-tRNA) *binding* sub-process, and *mechanochemical* sub-process during which ribosome will make a forward translocation step (i.e. one base pair). This model fits well to the recent experimental data obtained in [23]. Based on this model, properties of the ribosome translocation along mRNA, including its mean translocation rate and mean dwell time in one translocation cycle, are detailed discussed.

II. MODEL

As discussed in recent references [5, 6, 22, 23], the translocation of helicase along nucleic acid (DNA or RNA) might through two processes: active process and passive process, see Fig. 1. The main difference between these two processes is that, in active process, after completion of the necessary *translocation factor binding* processes, the junction of the two strains of the double-strained nucleic acid is effectively destabilized, and so the energy barrier for helicase to translocate to the next base is greatly reduced. But in the passive process, the helicase has to overcome a significant energy barrier, and so more time will be spent in waiting for the junction opening by thermal fluctuation. Biochemically, the free energy ΔG needed to open one base pair consists of the base-paring energy $\Delta G_{\rm bp}$, the destabilization energy of enzyme $\Delta G_{\rm d}$ and template stretching force ΔG_F, $\Delta G = \Delta G_{\rm bp} - \Delta G_{\rm d} - \Delta G_F$.

In both active process and passive process of ribosome translocation along mRNA, translocation factors EF-G•GTP and EF-Tu•GTP•aa-tRNA are needed [23, 37]. Therefore, there are at least two sub-processes in each of the two processes. For simplicity, we assume there are only two sub-processes in each translocation cycle: one *translocation factor binding* sub-process, and one *mechanochemical* sub-process during which one spatial mechanical translocation step is completed. Generally, all the four sub-processes (see Fig. 1): $\mathbf{1} \to \mathbf{2}$, $\mathbf{2} \to \mathbf{1}$ and $\mathbf{1'} \to \mathbf{3}$, $\mathbf{3} \to \mathbf{1'}$ might be reversible, for simplicity we assume in our model that they are all irreversible, with rate constants k_1, k_2 and k_1', k_3 respectively. $\mathbf{1} \to \mathbf{2} \to \mathbf{1}$ represents one active translocation step, and $\mathbf{1'} \to \mathbf{3} \to \mathbf{1'}$ represents one passive translocation step. As discussed in [23], $\mathbf{2} \to \mathbf{1}, \mathbf{3} \to \mathbf{1'}$ can be regarded as ribosome translocation through an open and closed nucleic acid fork, respectively. So k_3 depends only on the junction base pair, and k_2, k_3 are independent of external force. To reduce model parameters (and based on numerical tests), we assume that only the switch rate from passive process to active process is external force dependent, and the rates of *translocation factor binding* sub-process in both active ($\mathbf{1} \to \mathbf{2}$) and passive ($\mathbf{1'} \to \mathbf{3}$) processes are equal to each other, $k_1 = k_1'$, which depend only on the concentrations of translocation factors. Generally, the binding of translocation factors to ribosome might generate conformational change of the corresponding domain, which then might cause a little mechanical translocation. Here, for simplicity and to reduce the model parameters, we assume that the corresponding rates k_1, k_1' are independent of external force. Which means the whole mechanical step is made in the following *mechanochemical* sub-process. Meanwhile, we assume the switch rates between states $\mathbf{1}$ and $\mathbf{1'}$ are the same as those between states $\mathbf{2}$ and $\mathbf{3}$, i.e. $k_o' = k_o$ and $k_c' = k_c$. Under all these assumptions, the model illustrated in Fig. 1 is then reduced to the simple one illustrated in Fig. 2(a). To some extent, the model depicted in Fig. 2(a) is equivalent to the one depicted in Fig. 2(b). In this study, we will only discuss the model depicted in Fig. 2(a), since more information can be obtained from it but with the same parameter number as the one depicted in 2(b).

III. RESULTS

A. Mean translocation rate.

Let p_1, p_2 and ρ_1, ρ_2 be the probabilities that ribosome in states **1**, **2** and **1′**, **3** respectively, then one can easily show that they are governed the following master equations

$$\begin{aligned} dp_1/dt =& k_o\rho_1 + k_2p_2 - (k_1 + k_c)p_1, \\ dp_2/dt =& k_o\rho_2 + k_1p_1 - (k_2 + k_c)p_2, \\ d\rho_1/dt =& k_cp_1 + k_3\rho_2 - (k_1 + k_o)\rho_1, \\ d\rho_2/dt =& k_cp_2 + k_1\rho_1 - (k_3 + k_o)\rho_2. \end{aligned} \tag{1}$$

At steady state, one can easily get

$$\begin{aligned} p_1 &= k_o[k_2(k_1 + k_o) + k_3(k_2 + k_c)]/\Delta, \\ p_2 &= k_ok_1(k_1 + k_3 + k_c + k_o)/\Delta, \\ \rho_1 &= k_c[k_2(k_3 + k_o) + k_3(k_1 + k_c)]/\Delta, \\ \rho_2 &= k_ck_1(k_1 + k_2 + k_c + k_o)/\Delta, \end{aligned} \tag{2}$$

with the normalization constant $\Delta = (k_o + k_c)[(k_1 + k_2)(k_1 + k_3) + k_c(k_1 + k_3) + k_o(k_1 + k_2)]$. The mean translocation rate of ribosome can be obtained as follows

$$J = k_1(p_1 + \rho_1) = k_2p_2 + k_3\rho_2. \tag{3}$$

The ratio of probability $p := p_1 + p_2$ that ribosome stays in active process to probability $\rho := \rho_1 + \rho_2$ that in passive process is $p/\rho = k_o/k_c$. There is evidence that the ratio of switch rates k_o/k_c increases with external force [23], so under high external force, ribosome will translocate mainly by active process. One can easily show that the mean translocation rate of ribosome in active process is $J_a = k_1k_2/(k_1 + k_2)$, and the mean translocation rate in passive process is $J_b = k_1k_3/(k_1 + k_3)$. For low concentrations of translocation factors, i.e. k_1 is small, the mean translocation rate $J \approx k_1$, so the translocation is limited by the *translocation factor binding* process $\mathbf{1} \to \mathbf{2}$ or $\mathbf{1'} \to \mathbf{3}$. But for high concentration cases, i.e. k_1 is large enough, $J \approx (k_2k_o + k_3k_c)/(k_o + k_c)$, so the translocation is limited by the following *mechanochemical* process $\mathbf{2} \to \mathbf{1}$ or $\mathbf{3} \to \mathbf{1'}$. One can also show that, the ratio $(p_1 + \rho_1)/(p_2 + \rho_2)$ decreases with k_1, which means that for low concentration of translocation factor cases, ribosome mainly stays in states **1** or **1′**, but for high concentration cases, it is mainly in sates **2** or **3**. In one word, the external force determines which process, the active one $\mathbf{1} \to \mathbf{2} \to \mathbf{1}$ or the passive one $\mathbf{1'} \to \mathbf{3} \to \mathbf{1'}$, is the dominant process, while the concentrations of translocation factors determine which sub-process, the binding sub-process $\mathbf{1} \to \mathbf{2}$ ($\mathbf{1'} \to \mathbf{3}$) or the following *mechanochemical* sub-process $\mathbf{2} \to \mathbf{1}$ ($\mathbf{3} \to \mathbf{1'}$), limits the whole translocation of ribosome.

B. Mean dwell time.

The mean time that ribosome spent in one translocation cycle can be obtained as follows

$$T = p_1T_1 + p_2T_2 + \rho_1T_{1'} + \rho_2T_3. \tag{4}$$

Where $T_1, T_2, T_{1'}, T_3$ are the mean times spent by ribosome to complete one translocation cycle with initial states **1**, **2**, **1′**, **3**, respectively. T_1 satisfies the following equations [36, 38, 39]

$$\begin{aligned} T_1 &= \frac{1}{k_1+k_c} + \frac{k_1}{k_1+k_c}T_{12} + \frac{k_c}{k_1+k_c}T_{11'}, \\ T_{11'} &= \frac{1}{k_1+k_o} + \frac{k_o}{k_1+k_o}T_1 + \frac{k_1}{k_1+k_o}T_{13}, \\ T_{12} &= \frac{1}{k_2+k_c} + \frac{k_c}{k_2+k_c}T_{13}, \\ T_{13} &= \frac{1}{k_3+k_o} + \frac{k_o}{k_3+k_o}T_{12}. \end{aligned} \tag{5}$$

Where T_{1i} is the mean first passage time of ribosome from state **i** to state **1** or **1′** of the next translocation cycle [see Fig. 2(a)]. One can show that $T_1 = \Sigma_1/\Sigma$, with $\Sigma_1 = k_1(k_1+k_2+k_c+k_o)(k_3+k_c+k_o)+(k_c+k_o)(k_2k_3+k_3k_c+k_2k_o)$ and $\Sigma = k_1(k_2k_3+k_3k_c+k_2k_o)(k_1+k_c+k_o)$. The expressions of $T_2, T_{1'}, T_3$ can be obtained similarly. $T_{1'} = \Sigma_2/\Sigma$ with $\Sigma_2 = k_1(k_1+k_3+k_c+k_o)(k_2+k_c+k_o)+(k_c+k_o)(k_2k_3+k_2k_o+k_ck_3)$.

$$T_2 = \frac{(k_1+k_3)k_c + (k_1+k_2)(k_3+k_o)}{k_1(k_2k_3+k_3k_c+k_2k_o)} \tag{6}$$

and

$$T_3 = \frac{(k_1+k_2)k_o + (k_1+k_3)(k_2+k_c)}{k_1(k_2k_3+k_2k_o+k_3k_c)}. \tag{7}$$

C. Ribosome translocation along mRNA.

In the following, we will use the above model to discuss the external force and translocation factor concentration dependent properties of ribosome translocation along mRNA, which has been recently studied experimentally in [23]. As mentioned before, the switch rates of ribosome between active process and passive process depend on energy barrier of the strains junction $\Delta G = \Delta G_{\rm bp} - \Delta G_{\rm d} - \Delta G_F$. Under the assumption that $\Delta G_{\rm bp}$ and $\Delta G_{\rm d}$ are invariable in the translocation, the switch rates satisfy $k_o/k_c = \hat{k}_o^0/k_c^0 \exp(\delta\Delta G_F/k_BT)$. Here $0 \le \delta \le 1$ is an *energy distribution factor*, and numerical calculations indicate $\delta \lesssim 1$. For simplicity and reduction of model parameters (and also due to the test of numerical calculations), we assume $k_c = k_c^0$ is independent of external force. So

$$k_o = \hat{k}_o^0 \exp(\delta\Delta G_F/k_BT). \tag{8}$$

Another method which is usually used to account for the external force F dependence of transition rate is $k = k_0 \exp(F/F_0)$ with F_0 a constant [36, 40, 41]. This will be used in this study, i.e, we assume the external force dependence of switch rate k_o is as follows,

$$k_o = k_o^0 \exp(F/F_0). \tag{9}$$

In fact, the methods (8) and (9) are equivalent to each other for ribosome translocation process studied here. The reason is as follows. From the force-extension relation of DNA measured in [42] [or see 3(a)], the energy ΔG_F can be well approximated by $16F - 8$ for $F < 60$ pN, see Fig. 3(b) in which the thin solid line is from $\Delta G_F = 16F - 8$ and the thick dotted line is from $\Delta G_F = \int_0^F z(F)dF$ with $z(F)$ the extension as plotted in Fig. 3(a). So, by expressions (8) and (9), one can easily show that

$$\delta = \frac{k_BT}{16F_0}, \quad \hat{k}_o^0 = k_o^0 \exp\left(\frac{1}{2F_0}\right). \tag{10}$$

In the discussion below, we will always use expression (9), and the same results can also be obtained by method (8).

Generally, the rate k_3 of translocation in passive process should depend on the type of base pairs of the strains junction. Again, for the sake of simplicity, we always keep it constant [23]. Similarly, the transition rate k_2 in active process is also assume to be a constant. As studied in [23], there are at least two binding processes during sub-processes $\mathbf{1} \to \mathbf{2}$ or $\mathbf{1}' \to \mathbf{3}$, EF-G•GTP binding and EF-Tu•GTP•aa-tRNA binding. For simplicity, we assume there are only these two *translocation factor binding* processes (or all other translocation factors are held at saturating concentrations), and both of them are irreversible. Let $k_{11} = k_{11}^0$[EF-G] and $k_{12} = k_{12}^0$[EF-T] be the binding rates of EF-G•GTP and EF-Tu•GTP•aa-tRNA respectively. One can easily show that

$$k_1 = \frac{k_{11}k_{12}}{k_{11}+k_{12}} = \frac{k_{11}^0 k_{12}^0[\text{EF-G}][\text{EF-T}]}{k_{11}^0[\text{EF-G}] + k_{12}^0[\text{EF-T}]}. \tag{11}$$

With parameter values listed in Tab. I, the theoretical results of ribosome translocation rate J versus external force F and concentrations [EF-G], [EF-T] are plotted in Fig. 4, where the data points are from [23] for $\text{hpVal}_{\text{GC50}}$ mRNA. These plots indicate our model can explain the experimental data reasonably well. In Fig. 5(a), the curves for translocation rate J versus force F at saturating [EF-T] but various values of [EF-G] are plotted, and in Fig. 5(c), the curves for translocation rate J versus [EF-G] at saturating [EF-T] but various values of force F are plotted. From these two figures, one can easily see that, the translocation rate J increases monotonically with both force F and concentration [EF-G], but with one upper limit and one lower limit. Similar results can also be found for different values of [EF-T], see Fig. 5(b)(d). As mentioned before, at saturating concentration of translocation factors, the translocation of ribosome is limited by the *mechanochemical* sub-process $\mathbf{2} \to \mathbf{1}$ (or $\mathbf{3} \to \mathbf{1}'$), but at low concentration, it is limited by the *translocation factor binding* sub-process $\mathbf{1} \to \mathbf{2}$ (or $\mathbf{1}' \to \mathbf{3}$). Meanwhile, under high external force, ribosome translocates mainly through active process, but under low force, it is mainly through passive process. Actually, this can be demonstrated by Fig. 6. From Fig. 6(c), one sees that for any external forces, the probability $p_1+\rho_1$ of ribosome staying at state $\mathbf{1}$ or $\mathbf{1}'$ decreases with concentration [EF-G], which is because that the *translocation factor binding* rate k_1 increases with [EF-G]. However, the curves in Fig. 6(a) indicate that $p_1 + \rho_1$ increases with external force F, this is because that, with the increase of F ribosome will more like to reach state $\mathbf{1}$ (or $\mathbf{1}'$) by sub-process $\mathbf{2} \to \mathbf{1}$, which is fast than sub-process $\mathbf{3} \to \mathbf{1}'$ (see Tab. I for values of k_2 and k_3). This also can be seen from Fig. 6(b) that, the probability p_1+p_2 that ribosome translocates through active process increases monotonically with force F. Actually, numerical calculations show that this increase is almost exponential. The plots in Fig. 6(d) indicate p_1+p_2 is independent of concentration [EF-G]. In all the plots of Fig. 6, the concentration of [EF-T] is always held at a saturating concentration. Similar results can be obtained if [EF-T] is varied. Since all the sub-processes in our model are irreversible, and mean translocation rate J increases with both external force F and concentrations [EF-G], [EF-T], the mean dwell time T of ribosome in one translocation cycle decreases with both F and [EF-G], [EF-T], see Fig. 7.

IV. DISCUSSION

In this study, a model for ribosome translocation along messenger RNA is presented. In which, ribosome is assumed to translocate by two processes, active process and passive process. In each of the two processes, two sub-processes are included, *translocation factor binding* sub-process in which all the needed translocation factor are attached, and

mechanochemical sub-process in which one forward translocation step is made. The main difference between active process and passive process is that the transition rates of the *mechanochemical* sub-processes are different, which is due to the difference of free energy barrier. By this model, we found that, the mean translocation rate of ribosome increases with both the concentrations of translocation factors and the external force. Under high force, ribosome translocates mainly through active process, and at saturating concentrations of translocation factors, the translocation is limited by *mechanochemical* sub-processes. With the increase of external force, the mean translocation rate of ribosome increases from its lower limit to its upper limit. However, both of these two limits increase with concentrations of translocation factors.

Acknowledgments

This study is funded by the Natural Science Foundation of Shanghai (under Grant No. 11ZR1403700).

[1] S. C. West. DNA helicases: new breeds of translocating motors and molecular pumps. *Cell*, 86:177–180, 1996.

[2] T. M. Lohman and K. P. Bjornson. Mechanisms of helicase-catalysed unwinding. *Annu. Rev. Biochem.*, 65:169–214, 1996.

[3] M. R. Singleton, M. S. Dillingham, and D. B. Wigley. Structure and mechanism of helicases and nucleic acid translocases. *Annu. Rev. Biochem.*, 76:23–50, 2007.

[4] A. M. Pyle. Translocation and unwinding mechanisms of RNA and DNA helicases. *Annu. Rev. Biophys.*, 37:317–336, 2008.

[5] S. Kim, C. M. Schroeder, and X. S. Xie. Single-molecule study of DNA polymerization activity of HIV-1 reverse transcriptase on DNA templates. *J. Mol. Biol.*, 395:995–1006, 2010.

[6] M. Manosas, X. G. Xi, D. Bensimon, and V. Croquette. Active and passive mechanisms of helicases. *Nucleic Acids Research*, 38:5518–5526, 2010.

[7] S. Dumont, W. Cheng, Vi. Serebrov, R. K. Beran, I. Tinoco Jr, A. M. Pyle, and C. Bustamante. RNA translocation and unwinding mechanism of HCV NS3 helicase and its coordination by ATP. *Nature*, 439:105–108, 2006.

[8] J.-B. Lee, R. K. Hite, S. M. Hamdan, X. S. Xie, C. C. Richardson, and A. M. van Oijen. DNA primase acts as a molecular brake in DNA replication. *Nature*, 439:621–624, 2006.

[9] W. Cheng, S. Dumont, I. Tinoco, and C. Bustamante. NS3 helicase actively separates RNA strands and senses sequence barriers ahead of the opening fork. *Proc. Natl. Acad. Sci. USA*, 104:13954–13959, 2007.

[10] S. Myong, M. M. Bruno, A. M. Pyle, and T. Ha. Spring-loaded mechanism of DNA unwinding by hepatitis C virus NS3 helicase. *Science*, 317:513–516, 2007.

[11] D. S. Johnson, L. Bai, B. Y. Smith, S. S. Patel, and M. D. Wang. Single molecule studies reveal dynamics of DNA unwinding by the ring-shaped t7 helicase. *Cell*, 129:1299–1309, 2007.

[12] W. Cheng, S. G. Arunajadai, J. R. Moffitt, I. Tinoco Jr., and C. Bustamante. Singlecbase pair unwinding and asynchronous RNA release by the hepatitis C virus NS3 helicase. *Science*, 333:1746–1749, 2011.

[13] F. Rozen, I. Edery, K. Meerovitch, T. E. Dever, W. C. Merrick, and N. Sonenberg. Bidirectional RNA helicase activity of eucaryotic translation initiation factors 4A and 4F. *Mol. Cell. Biol.*, 10:1134–1144, 1990.

[14] S. B. Smith, Y. Cui, and C. Bustamante. Moverstretching B-DNA: The elastic response of individual double-stranded and single-stranded DNA molecules. *Science*, 271:795–799, 1996.

[15] U. Bockelmann, B. Essevaz-Roulet, and F. Heslot. Molecular stick-slip motion revealed by opening dna with piconewton forces. *Phys. Rev. Lett.*, 79:4489–4492, 1997.

[16] B. Essevaz-Roulet, U. Bockelmann, and F. Heslot. Mechanical separation of the complementary strands of DNA. *Proc. Natl. Acad. Sci. USA*, 94:11935–11940, 1997.

[17] M. D. Wang, H. Yin, R. Landick, J. Gelles, and S. M. Block. Stretching DNA with optical tweezers. *Biophys. J.*, 72:1335–1346, 1997.

[18] S. Takyar, R. P. Hickerson, and Harry F. Noller. mRNA helicase activity of the ribosome. *Cell*, 120:49–58, 2005.

[19] J. Gore, Z. Bryant, M. Nöllmann, M. U. Le, , N. R. Cozzarelli, and C. Bustamante. DNA overwinds when stretched. *Nature*, 442:836–839, 2006.

[20] J.-D. Wen, L. Lancaster, C. Hodges, A.-C. Zeri, S.-H. Yoshimura, H. F. Noller, C. Bustamante, and Jr. I. Tinoco. Following translation by single ribosomes one codon at a time. *Nature*, 452:598–603, 2008.

[21] I. Donmez and S. S. Patel. Coupling of DNA unwinding to nucleotide hydrolysis in a ring-shaped helicase. *EMBO J.*, 27:1718–1726, 2008.

[22] M. D. Betterton and F. Julicher. Opening of nucleic-acid double strands by helicases: active versus passive opening. *Phys. Rev. E*, 71:11904–11911, 2005.

[23] X. Qu, J.-D. Wen, L. Lancaster, H. F. Noller, C. Bustamante, and I. Tinoco Jr. The ribosome uses two active mechanisms to unwind messenger RNA during translation. *Nature*, 475:118–121, 2011.

[24] S. S. Velankar, P. Soultanas, M. S. Dillingham, H. S. Subramanya, and D. B. Wigley. Crystal structures of complexes of PcrA DNA helicase with a DNA substrate indicate an inchworm mechanism. *Cell*, 97:75–84, 1999.

[25] M. K. Levin, M. M. Gurjar, and S. S. Patel. A Brownian motor mechanism of translocation and strand separation by hepatitis c virus helicase. *Nat. Struct. Mol. Biol.*, 12:429–435, 2005.

[26] M. D. Betterton and F. Julicher. Velocity and processivity of helicase unwinding of double-stranded nucleic acids. *J. Phys.: Condens. Matter*, 17:S3851, 2005.

[27] S. S. Patel and I. Donmez. Mechanisms of helicases. *J. Bio. Chem.*, 281:18265–18268, 2006.

[28] J. Yu, T. Ha, and K. Schulten. Structure-based model of the stepping motor of PcrA helicase. *Biophys. J.*, 91:2097–2114, 2006.

[29] T. Lionnet, M. M. Spiering, S. J. Benkovic, D. Bensimon, and V. Croquette. Real-time observation of bacteriophage T4 gp41 helicase reveals an unwinding mechanism. *Proc. Natl. Acad. Sci. USA*, 104:19790–19795, 2007.

[30] B. Sun, K.-J. Wei1, B. Zhang, X.-H. Zhang, S.-X. Dou, M. Li, and X. G. Xi. Impediment of E. coli UvrD by DNA-destabilizing force reveals a strained-inchworm mechanism of DNA unwinding. *EMBO J.*, 27:3279–3287, 2008.

[31] A. Garai, D. Chowdhury, and M. D. Betterton. Two-state model for helicase translocation and unwinding of nucleic acids. *Phys. Rev. E*, 77:061910, 2008.

[32] I. Tinoco and J.-D. Wen. Simulation and analysis of single-ribosome translation. *Phys. Biol.*, 6:025006, 2009.

[33] M. Gu and C. M. Rice. Three conformational snapshots of the hepatitis C virus NS3 helicase reveal a ratchet translocation mechanism. *Proc. Natl Acad. Sci. USA*, 107:521–528, 2010.

[34] Jin Yu, Wei Cheng, Carlos Bustamante, and George Oster. Coupling translocation with nucleic acid unwinding by NS3 helicase. *J. Mol. Biol.*, 404:439–455, 2010.

[35] B. Akiyoshi, K. K. Sarangapani, A. F. Powers, C. R. Nelson, S. L. Reichow, H. Arellano-Santoyo, T. Gonen, J. A. Ranish, C. L. Asbury, and S. Biggins. Tension directly stabilizes reconstituted kinetochore-microtubule attachments. *Nature*, 468:576–579, 2010.

[36] Y. Zhang. Growth and shortening of microtubules: A two-state model approachr. *The Journal Of Biological Chemistry*, 286:39439–39449, 2011.

[37] M. V. Rodnina, A. Savelsbergh, V. I. Katunin, and W. Wintermeyer. Hydrolysis of GTP by elongation factor G drives

tRNA movement on the ribosome. *Nature*, 385:37–41, 1997.

[38] Y. Zhang. An effective description of periodic one-dimensional hopping model. *Science in China Series G*, 54:401–405, 2011.

[39] Yunxin Zhang. Periodic one-dimensional hopping model with transitions between nonadjacent states. *Phys. Rev. E*, 84:031104, 2011.

[40] George I. Bell. Models for the specific adhesion of cells to cells. *Science*, 200:618–627, 1978.

[41] M. J. I. Müller, S. Klumpp, and R. Lipowsky. Tug-of-war as a cooperative mechanism for bidirectional cargo transport by molecular motors. *Proc. Natl. Acad. Sci. USA*, 105:4609–4614, 2008.

[42] I. Tinoco and C. Bustamante. The effect of force on thermodynamics and kinetics of single molecule reactions. *Biophys. Chem.*, 101-102:513–533, 2002.

TABLE I: Values of model parameters used in Figs. 4-7, which are obtained by fitting formulation (3) of mean translocation rate of ribosome along mRNA to the experimental data obtained in [23] (see Fig. 4). See also Fig. 2(a) and Eqs.(1), (9), (11) for definitions of the model parameters.

Parameter	Value	Parameter	Value
k_{11}	13.78 ($s^{-1} \cdot \mu M^{-1}$)	k_{12}	106.85 ($s^{-1} \cdot \mu M^{-1}$)
k_2	0.44 (codons$\cdot s^{-1}$)	k_3	0.26 (codons$\cdot s^{-1}$)
k_o^0	8.66×10^{-9} (s^{-1})	k_c^0	41.28 (s^{-1})
F_0	0.66 (pN)		

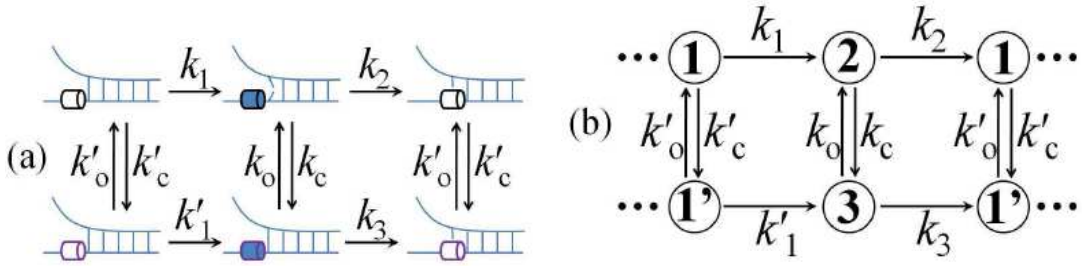

FIG. 1: Schematic depiction of the general model to describe helicase translocation along nucleic acid (a) and its corresponding two-line Markov chain (b). There are two possible processes to complete one step, active process (top, $\mathbf{1} \to \mathbf{2} \to \mathbf{1}$) and passive process (down, $\mathbf{1}' \to \mathbf{3} \to \mathbf{1}'$), with different *translocation factor binding* rates and *mechanochemical* transition rates k_1, k_2 and k_1', k_3, respectively. These two processes can switch to each other with external force and state dependent rates, k_o, k_c, k_o', k_c'. The needed translocation factors are attached during sub-process $\mathbf{1} \to \mathbf{2}$ or $\mathbf{1}' \to \mathbf{3}$, and one forward step is completed during sub-process $\mathbf{2} \to \mathbf{1}$ or $\mathbf{3} \to \mathbf{1}'$.

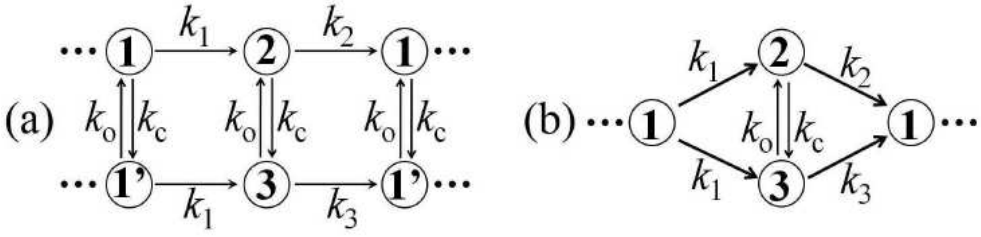

FIG. 2: Simplifications of the model depicted in Fig. 1. (a) The switch rates between active process and passive process are assumed to be state independent, $k_o' = k_o$ and $k_c' = k_c$, and the rates of *translocation factor binding* sub-process in both active process and passive process are also assumed to be the same, $k_1' = k_1$. (b) states $\mathbf{1}$ and $\mathbf{1}'$ are combined to one state, and $k_1' = k_1$ is assumed. Since the parameter numbers of the two simplified models are the same, but more information can be obtained from the one depicted in (a), in this study only the simplified model (a) is analyzed.

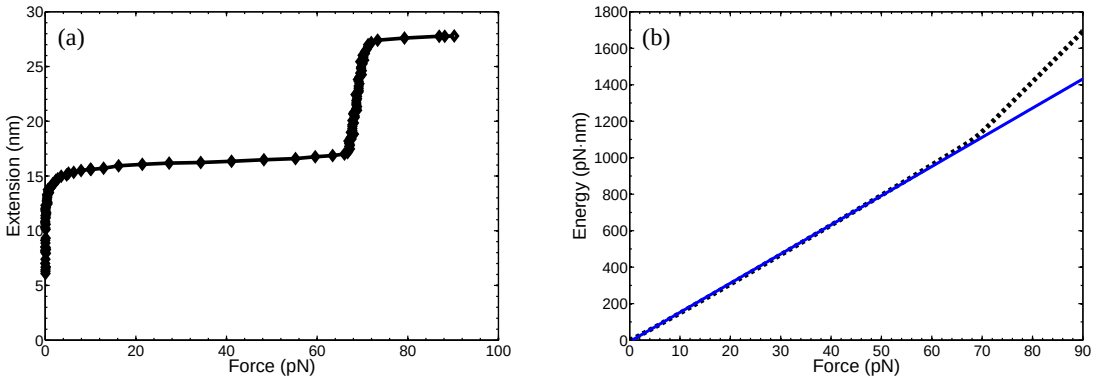

FIG. 3: (a) The extension-force relation of DNA obtained by Tinoco and Bustamante in [42]. (b) The free energy-force relation obtained by $\Delta G_F = \int_0^F z(F)dF$ (thick dotted line) with $z(F)$ the total extension under force F as plotted in (a). For $F < 60$, ΔG_F can be well approximated by $16F - 8$ (thin solid line).

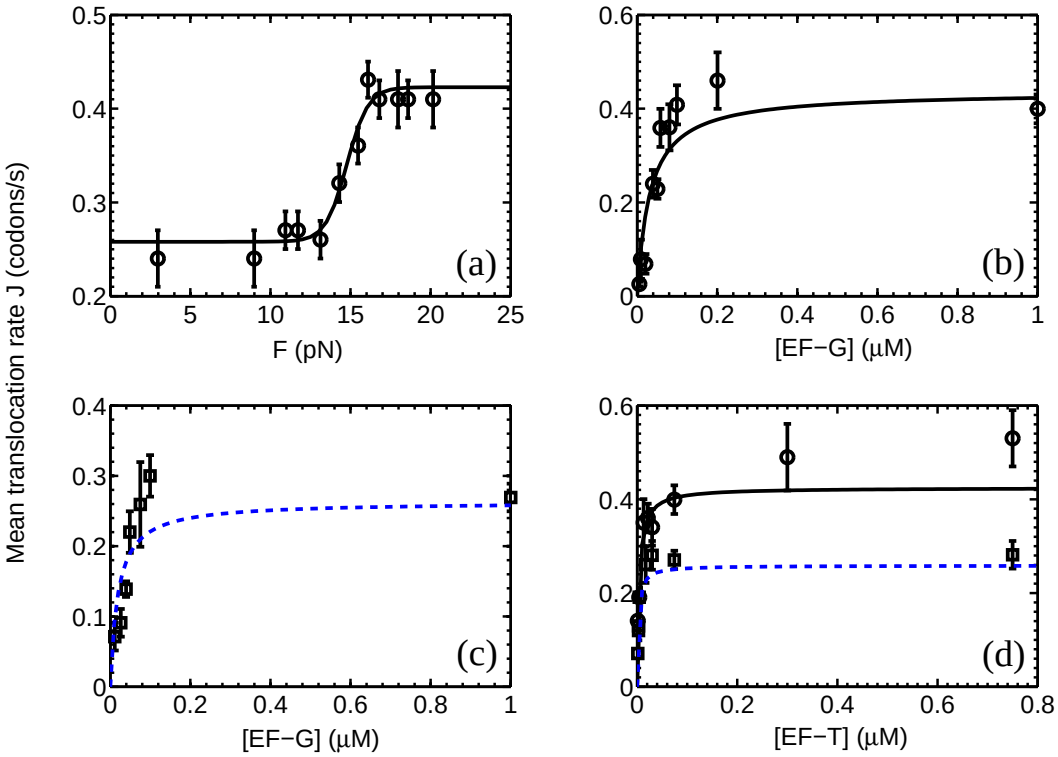

FIG. 4: Theoretical results of ribosome translocation along hpVal$_{GC50}$ mRNA [see Eqs. (2) (3) (9) and (11)] with parameter values listed in Tab. I. The data points are experimentally obtained by Qu, *et al* [23]. In (b) (c) and (d), the solid curves are mean translocation rate J under high external force ($F = 20$ pN is used in the calculations), and dashed curves are values for low external force ($F = 2$ pN is used in the calculations). In (a) [EF-G]=[EF-T]=1 μM is used.

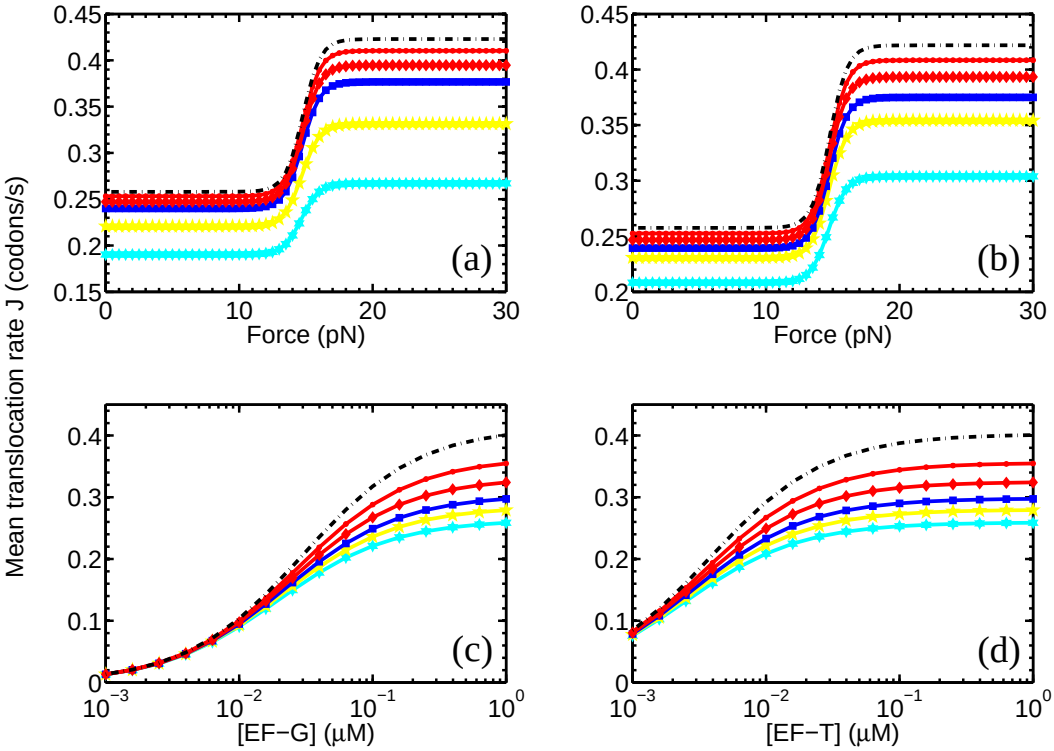

FIG. 5: Mean translocation rate J of ribosome along hpVal$_{\mathrm{GC50}}$ bmRNA (see [23]) as functions of external force F, concentrations [EF-G] and [EF-T]. Parameter values used in the calculations are as follows. (a) [EF-T]=1 μM, and reading from the bottom up [EF-G]=0.05, 0.1 0.2, 0.3, 0.5, and 1 μM respectively. (b) [EF-G]=1 μM, and reading from the bottom up [EF-T]=0.01, 0.02, 0.03, 0.05, 0.1, and 0.6 μM respectively. (c) [EF-T]=1 μM and (d) [EF-G]=1 μM. In (c) (d), reading from the bottom up, external force F =11, 13.5, 14, 14.5, 15, and 16 pN respectively. Other parameter values are listed in Tab. I. The calculations indicate that the mean translocation rate J increases with both external force F and concentrations [EF-G], [EF-T].

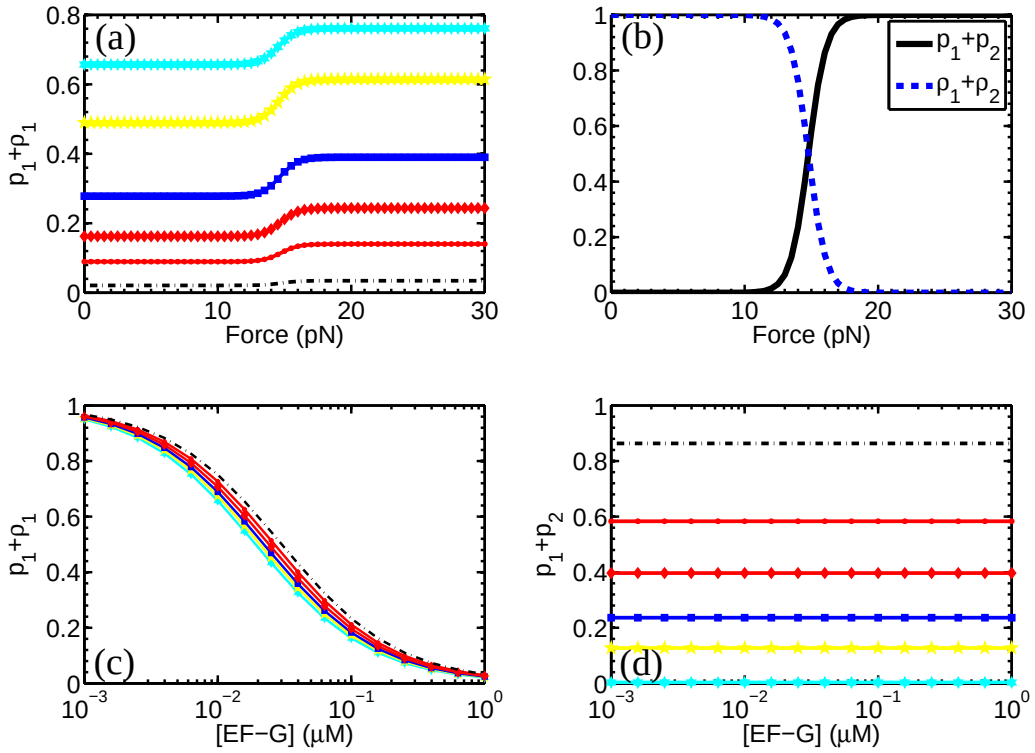

FIG. 6: Probability $p_1 + \rho_1$ of ribosome at state **1** or **1**′ [see Fig. 2(a)] as function of external force F (a) and concentration [EF-G] (c). (b) (d) are for probability $p_1 + p_2$ of ribosome at state **2** or **3**. The parameter values used in the calculations are as follows. (a) [EF-T]=1 μM, and reading from top downwards [EF-G]=0.01, 0.02 0.05, 0.1, 0.2 and 1 μM respectively. (b)[EF-G]=[EF-T]=1 μM, the curves are independent of [EF-G] and [EF-T]. (c) (d) [EF-T]=1 μM, and reading from the bottom up F =11, 13.5, 14, 14.5, 15, 16 pN respectively. For other parameter values, see Tab. I.

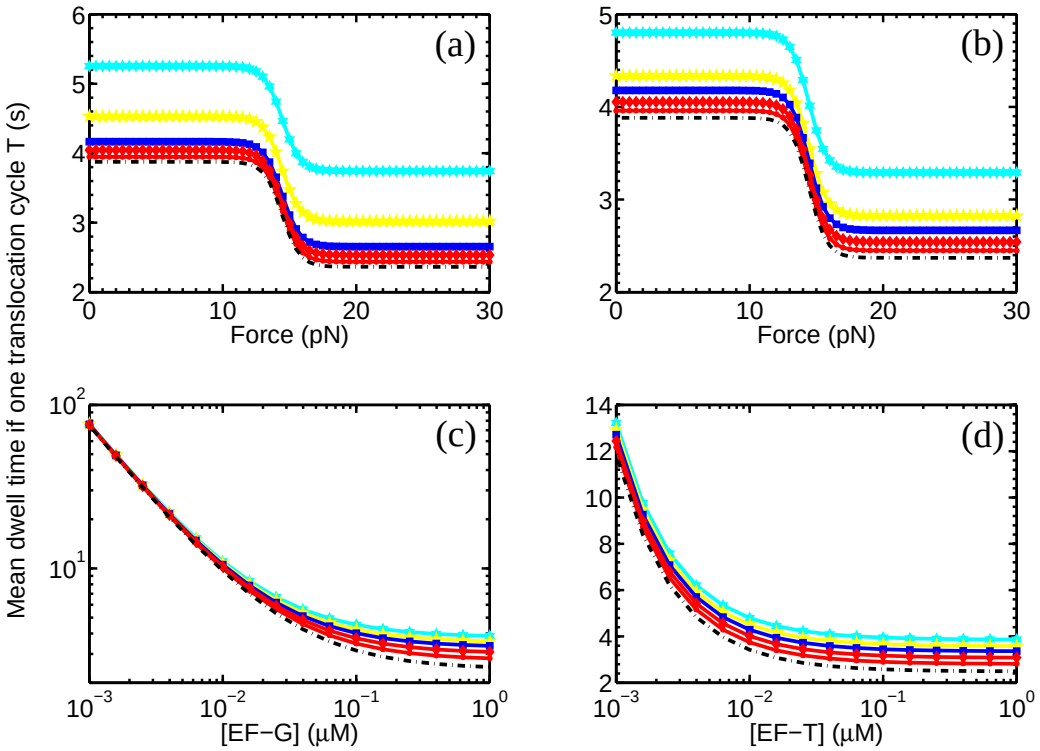

FIG. 7: Mean dwell time of ribosome in one translocation cycle as the change of external force [see (a) and (b)], concentrations of EF-G•GTP [see (c)] and EF-Tu•GTP•aa-tRNA [see (d)]. In addition to the parameter values listed in Tab. I, others are as follows. (a) [EF-T]=1 μM, and reading from top downwards [EF-G]=0.05, 0.1, 0.2, 0.3, 0.5 and 1 μM respectively. (b) [EF-G]=1 μM, and reading from top downwards [EF-T]=0.01, 0.02, 0.03, 0.05, 0.1, and 0.6 μM respectively. (c) [EF-T]=1 μM, and (d) [EF-D]=1 μM. In both (c) and (d), reading from top downwards F =11, 13.5, 14, 14.5, 15, 16 pN respectively.